Ultrafast Rabi flopping in a three-level energy ladder

Jongseok Lim, Kanghee Lee, and Jaewook Ahn*

Department of Physics, KAIST, Daejeon 305-701, South Korea

**Corresponding author: jwahn@kaist.ac.kr*

Received June 5, 2012; revised July 13, 2012; accepted July 13, 2012;
posted July 16, 2012 (Doc. ID 169200); published August 8, 2012

We demonstrate Rabi oscillation of a resonant two-photon transition in a three-level ladder-type quantum system of gaseous rubidium atoms induced by a single femtosecond laser pulse. For this, we shape the flat-top spatial profile of the laser pulse and perform the ultrafast population cycling of the atoms as a function of pulse energy. The experimental result confirms that the Rabi frequency of the transition from a ground state to a final state depends linearly on the pulse area, although the transition is a two-photon process.

OCIS codes: 320.5540, 020.1670, 320.0320.

Coherent manipulation of a quantum system by light is substantial fulfillment for the implementation of quantum information processing [1,2]. For the coherence control of quantum dynamics, the use of the ultrafast laser technique and its time-resolved capability has attracted considerable interest because of its potential applications for quantum gate operations in femtosecond time scale [3–5]. In particular, the coherence control among the broad spectral components of ultrafast laser pulses as well as their coherent interaction with quantum systems enables implementation of on-demand quantum interferences among multiple transition passages of the systems and, thereby, provides a powerful optical means of quantum state preparations, especially, in multilevel systems [6–10].

As an example of ultrafast coherent control of multilevel quantum system, we consider optical Rabi flopping [11], a notably important feature in quantum control and quantum computing and, therefore, studied and used extensively in quantum systems ranging from atoms and molecules to semiconductors and nanomaterials [12–18]. Optical Rabi flopping, or optical Rabi oscillation, is an oscillatory behavior of the transition probability occurring in the coherent interaction regime of an oscillatory optical field with a two-level quantum system [11], and the transition probability alternates from zero to unity at a Rabi frequency $\Omega(t) = \mu A(t)/\hbar$, where μ is the coupling strength between the states and $A(t)$ is the electric field envelope. Although optical Rabi flopping has been widely studied with continuous, or quasi-monochromatic pulsed, electric fields, ultrafast laser pulses have only recently been considered with multilevel system experiments [12].

In this Letter, we present an experimental demonstration of Rabi oscillation in the resonant two-photon transition of a three-level ladder-type quantum system. The system under consideration comprises a ground energy state $|g\rangle$, an intermediate energy state $|i\rangle$, and a final energy state $|f\rangle$. When both the transitions $|g\rangle \rightarrow |i\rangle$ and $|i\rangle \rightarrow |e\rangle$ are resonantly driven simultaneously by a single laser pulse of a finite spectral bandwidth, (i.e., the two-photon transition $|g\rangle \rightarrow |f\rangle$ is strongly coupled with the resonant intermediate energy state $|i\rangle$), Rabi oscillation can occur collectively among the constituent energy states in this energy level configuration. The bare Rabi frequency Ω_{gi}, between $|g\rangle$ and $|i\rangle$, is shifted due to the presence of the interaction with $|f\rangle$, and likewise the two-photon Rabi frequency Ω_{gf}, between $|g\rangle$ and $|f\rangle$ via $|i\rangle$, becomes exactly the double of the shifted one-photon Rabi frequency Ω'_{gi}. The transition probability amplitude from $|g\rangle$ to $|f\rangle$ via $|i\rangle$ can be obtained from the time-dependent Schrödinger equation [19,20] as

$$c_{fg} = -\frac{2\Theta_{fi}\Theta_{ig}}{\Theta_{ig}^2 + \Theta_{fi}^2} \sin^2 \frac{1}{2}\sqrt{\Theta_{ig}^2 + \Theta_{fi}^2}, \tag{1}$$

where $\Theta_{ig,fi} = \int_{-\infty}^{\infty} \mu_{ig,fi} A(t)/\hbar dt'$ are the pulse areas and $\mu_{ig,fi}$ are the dipole moments between $|g\rangle$ and $|i\rangle$, and $|i\rangle$ and $|f\rangle$, respectively. It is worth noting that, despite the fact that the given transition is two-photon process, the oscillation frequency in Eq. (1), $\Theta_{\text{total}} = \frac{1}{2}\sqrt{\Theta_{ig}^2 + \Theta_{fi}^2}$, depends not on the intensity, but on the electric field, or the pulse area.

Experiments were performed with rubidium (Rb) atomic vapor, and the three-level energy-ladder system consisted of the $5S_{1/2}$, $5P_{3/2}$, and 5D energy states that correspond to the ground, the intermediate, and the final states, respectively (see Fig. 1). The coherent transition of $5S_{1/2} \rightarrow 5P_{3/2} \rightarrow 5D$ was achieved via two-photon absorption of ultrafast laser pulses. We used a Ti:sapphire laser amplifier system producing 35 fs pulses with a pulse energy of up to 500 μJ at a repetition rate of 1 kHz. The spectrum of the laser was centered at 778 nm with spectral width of 26 nm.

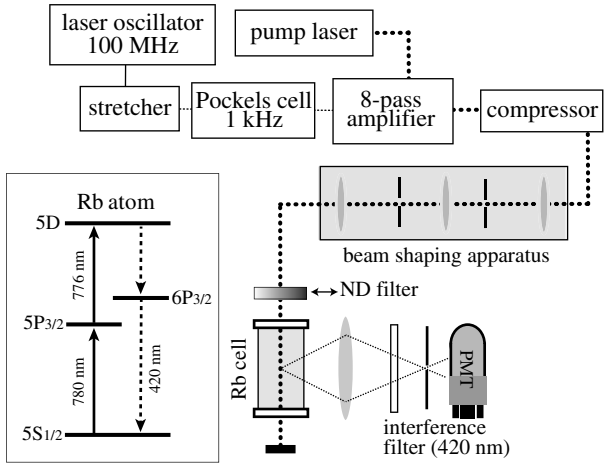

Fig. 1. Schematic of the experimental setup. The inset shows the energy level diagram.

Generic Gaussian laser pulses do not exhibit Rabi oscillation, but rather a monotonic increasing behavior, when interacting with uniformly distributed atoms, because of the spatial averaging effect resulting from the electric field distribution in transverse direction. Therefore, the laser beam profile needs to be modified to a flat-top. In our experiment, the flat-top spatial profile was implemented by a beam shaping apparatus that imaged a clipped Gaussian beam with finite-size lenses, and the interference between the diffraction fringe of the clipped Gaussian laser beam resulted in the flat-top profile. As shown in Fig. 2, the Gaussian beam was first spatially filtered with a pinhole with a diameter of 100 μm at the focus of a 4 : 1.5 telescope; the first and the second lenses in the apparatus have focal lengths of 400 and 150 mm, respectively. The rim of the beam was then clipped with a variable aperture, and the clipped beam profile was imaged onto the measurement spot with a lens of $f = 200$ mm focal length and $D = 25.4$ mm diameter. The imaged spot had a diameter of $d = 200$ μm, and its distance from the lens was $R = 1.4f$ (i.e., the magnification was about 0.4). According to Fourier optics theory [21], the focused beam shape $U_f(x, y)$ at the measurement spot is given by

$$U_f(x, y) = \tilde{h}(x, y) \otimes U_i(x, y), \tag{2}$$

where $\tilde{h}(x, y)$ is the point-spread function of imaging and $U_i(x, y)$ is the spatial profile of the clipped Gaussian beam. As $\tilde{h}(x, y)$ of a finite lens is determined by an Airy disk with its extent given by $1.22R\lambda/D$, with the given focal lengths of the lenses and the pinhole diameter, which are chosen in avoidance of the nonlinear effect at the beam focal point, numerical calculation predicts that the flat factor $\langle \Delta I \rangle / \langle I \rangle$ of a less than 3.5% is achieved when $d \approx 10R\lambda/D$ is satisfied (i.e., about 10 Airy side lobes cover the focused spot).

The constructed beam profile was first tested with a charged coupled device (CCD) camera, which temporally replaced the Rb cell. The recorded spot was located at the center of the Rb cell and also in the image plane of our beam shaping apparatus. Figure 2(a) shows the flat-top beam profile recorded with the CCD. The intensity distribution shown in Fig. 2(b) indicates that the intensity distribution was concentrated within ±5% range. For comparison, the transverse intersections of the beam center of the flat-top beam and the unclipped Gaussian beam are both plotted in Fig. 2(c). As a result, a flat-top beam of 200 μm size, which corresponded to the half of the Gaussian width of the unclipped beam, was constructed. It is noted that the intensity at the beam center was slightly lowered due to the interference, and the intensities of the edge were slightly increased. Furthermore, the broadband nature of the ultrafast pulse removed local intensity spikes, which remained in the numerical simulation carried out with a monochromatic source.

The experimental result of ultrafast Rabi flopping performed with the laser pulses of the prepared flat-top spatial profile is shown in Fig. 3. The population of the 5D state was measured as a function of pulse energy by detecting the fluorescence signal decayed from $6P_{3/2}$ to $5S_{1/2}$ with a photomultiplier tube (PMT) passing

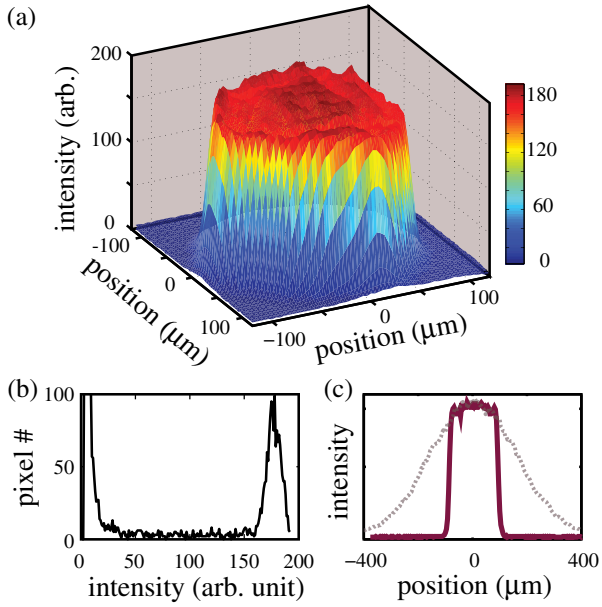

Fig. 2. (Color online) (a) Spatial profile and (b) intensity distribution of the constructed flat-top laser pulse; (c) intersections of the flat-top and Gaussian beam profiles.

through a 10 nm band-pass interference filter centered at 420 nm. We collected the fluorescence signal only from the flat-top region of 200 μm diameter using an imaging apparatus consisting of a 50 mm focal length lens and a 1 mm diameter aperture. It is noted that the DC-like increasing behavior of the experiment resulting from the back reflection at the exit surface of the Rb cell was subtracted by filtering out the lower frequency components less than one tenth of the observed oscillation. The pulse energy was varied by translating a variable neutral density (ND) filter (optical density is from 2.0 to 0.04) from 0.4 to 40 μJ, whose variation corresponds to 3.5 Rabi cycles of Θ_{total} in Eq. (1).

The 5D population measurement, depicted with brown squares in Fig. 3, is compared with the calculations. The numerical calculation (gray dashed line) of the time-dependent Schrödinger equation under the assumptions of rotating wave approximation (RWA) and a uniform

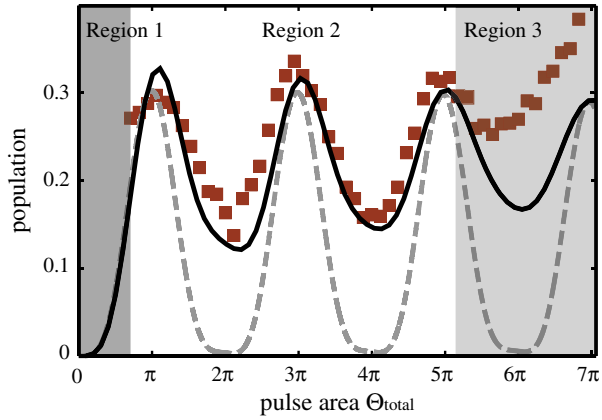

Fig. 3. (Color online) Experimental results (brown squares) of the 5D population plotted as a function of pulse area. For comparison, the numerical model calculation (gray dashed line), and the refined numerical calculation (black line), which takes the actual beam profile into account.

laser intensity predicts that the oscillatory behavior and its period are in accordance with the measurement. Further, when we take into account the intensity distribution of the actual laser beam measured in Fig. 2(b), the refined numerical calculation (black solid line) shows a good agreement with the experimental result. It is noted that the linear response region (region 2 in Fig. 3) starts from the pulse area of 0.7π due to the maximal optical density (2.0) of the ND filter, and the experimental data in region 1 was not obtained. The deviation of the Rabi oscillation from the simple sinusoidal shape in region 3 was not due to the Bloch–Siegert shift (i.e., no RWA), as this shift was under 5% of the oscillation frequency for the highest intensity in our experiment. The Rb atom density was 7×10^9 cm^{-3}, so the atom number in the interaction volume of 3×10^{-5} cm^3 was 2×10^5. Therefore, the experimental condition did not reach the superfluorescence threshold [22]. Also, because the oscillation behavior could be significantly affected from the spectral phases, the laser pulses were strictly kept in Fourier transform limit by checking the spectral chirp with a self-diffraction-type FROG [23]. The measured linear chirp value was less than 100 fs^2. It is speculated that the combined effects of dynamic Stark shift and the $5P_{1/2} \rightarrow 5D_{3/2}$ transition contributed to the experiment and the simple three-level model failed in region 3.

In summary, we have considered the Rabi oscillation of a resonant two-photon transition, appearing in the ultrafast optical interaction with a three-level energy-ladder system. By shaping the beam profile from Gaussian to flat-top, the interaction between the laser pulse and the gaseous atomic Rubidium has been performed at constant electric field at a given laser pulse energy, and the 3.5 cycles of oscillatory ultrafast Rabi flopping within the 35 fs pulse duration have been clearly observed.

This research was supported by Basic Science Research and Mid-career Researcher Programs through the National Research Foundation of Korea (NRF) funded by the Ministry of Education, Science, and Technology (2009-0090843 and 2010-0013899).

References

1. M. A. Nielson and I. L. Chuang, *Quantum Computation and Quantum Information* (Cambridge University, 2010).
2. P. Kok and B. W. Lovett, *Introduction to Optical Quantum Information Processing* (Cambridge University, 2010).
3. W. C. Campbell, J. Mizrahi, Q. Quraishi, C. Senko, D. Hayes, D. Hucul, D. N. Matsukevich, P. Maunz, and C. Monroe, Phys. Rev. Lett. **105**, 090502 (2010).
4. X. Li, Y. Wu, D. Steel, D. Gammon, T. H. Stievater, D. S. Katzer, D. Park, C. Piermarocchi, and L. J. Sham, Science **301**, 809 (2003).
5. A. Eckstein, B. Brecht, and C. Silberborn, Opt. Express **19**, 13770 (2011).
6. K. Bergmann, H. Theuer, and B. W. Shore, Rev. Mod. Phys. **70**, 1003 (1998).
7. M. Shapiro and P. Brumer, *Principles of the Quantum Control of Molecular Processes* (Wiley, 2003).
8. S. D. Clow, C. Trallero-Herrero, T. Bergeman, and T. Weinacht, Phys. Rev. Lett. **100**, 233603 (2008).
9. J. Lim, H. Lee, J. Kim, S. Lee, and J. Ahn, Phys. Rev. A **83**, 053429 (2011).
10. S. Lee, J. Lim, C. Y. Park, and J. Ahn, Opt. Express **19**, 2266 (2011).
11. L. Allen and J. H. Eberly, *Optical Resonance and Two-level Atoms* (Wiley, 1975).
12. S. Zhdanovich, J. W. Hepburn, and V. Miler, Phys. Rev. A **84**, 053428 (2011).
13. K. C. Nowack, F. H. L. Koppens, Yu. V. Nazarov, and L. M. K. Vandersypen, Science **318**, 1430 (2007).
14. I. Chiorescu, Y. Nakamura, C. J. P. M. Harmans, and J. E. Mooij, Science **299**, 1869 (2007).
15. H. Htoon, T. Takagahara, D. Kulik, O. Baklenov, A. L. Holmes, Jr., and C. K. Shih, Phys. Rev. Lett. **88**, 087401 (2002).
16. S. Stufler, P. Machnikowski, P. Ester, M. Bichler, V. M. Axt, T. Kuhn, and A. Zrenner, Phys. Rev. B **73**, 125304 (2006).
17. H. Choi, V.-M. Gkortsas, L. Diehl, D. Bour, S. Corzine, J. Zhu, G. Höfler, F. Capasso, F. X. Kärtner, and T. B. Norris, Nat. Photon. **4**, 706 (2010).
18. C.-M. Simon, T. Belhadj, B. Chatel, T. Amand, P. Renucci, A. Lemaitre, O. Krebs, P. A. Dalgarno, R. J. Warburton, X. Marie, and B. Urbaszek, Phys. Rev. Lett. **106**, 166801 (2011).
19. M. Sargent III and P. Horwitz, Phys. Rev. A **13**, 1962 (1976).
20. A. F. Linskens, I. Holleman, N. Dam, and J. Reuss, Phys. Rev. A **54**, 4854 (1996).
21. J. W. Goodman, *Introduction to Fourier Optics*, 3rd ed. (Roberts & Company, 2005).
22. E. Paradis, B. Barrett, A. Kumarakrishnan, R. Zhang, and G. Raithel, Phys. Rev. A **77**, 043419 (2008).
23. D. J. Kane and R. Trebino, IEEE J. Quantum Electron. **29**, 571 (1993).